Upregulated miR-378a-3p expression suppresses energy metabolism and promotes apoptosis by targeting a GLUT-1/ALDOA/PKM2 axis in esophageal carcinoma

YUAN QU[1*], SHAN XUE[2*], YUJIAN ZHENG[1], YAJING DU[2], GUOPING ZHANG[3], LITING HUANG[2], HUI LI[4] and HUIWU LI[2]

[1]Department of Labour Hygiene and Sanitary Science, College of Public Health, Xinjiang Medical University, Urumqi, Xinjiang 830011; [2]Medical Research Center; [3]Tumor Department, Yuebei People's Hospital, Shantou University, Shaoguan, Guangdong 512025; [4]Central Laboratory of Xinjiang Medical University, Xinjiang Medical University, Urumqi, Xinjiang 830011, P.R. China

Received August 24, 2022; Accepted July 10, 2023

DOI: 10.3892/ol.2023.14007

Abstract. Esophageal squamous cell carcinoma (ESCC) is an aggressive malignancy of the digestive system with increasing incidence and mortality rates. The biological roles of microRNA (miR)-378a-3p in tumor cells remain contested, and the mechanisms underlying the functions, energy metabolism, and cell survival mechanisms in ESCC cells are yet to be fully elucidated. In the present study, miR-378a-3p overexpression and negative control plasmids were transfected into ECA-109 cells using electroporation. Western blotting was used to detect the relative expression of proteins, and flow cytometry was used to detect cell apoptosis. Subsequently, ELISA assays were performed to determine enzyme activity, and an ATP detection kit was used to measure ATP content. Dual-luciferase reporter assays were performed to identify the target genes of miR-378a-3p. The results of the present study demonstrated that miR-378a-3p inhibited the gene expression and enzyme activities of glucose transporter protein 1 (GLUT-1), Aldolase A (ALDOA), and pyruvate kinase M2 (PKM2), all of which are involved in the glycolytic pathway of cells. Energy metabolism was suppressed by miR-378a-3p by reducing ATP content, and this downregulated the expression of Bcl-2 and Survivin. Moreover, increased miR-378a-3p expression promoted cell apoptosis in the early stages by increasing the expression levels and the activity of Bad and Caspase-3, while inhibiting the expression levels of Bcl-2 and Survivin. The results of the present study also demonstrated that GLUT-1/ALDOA/PKM2 were target genes of miR-378a-3p. Notably, miR-378a-3p blocked energy production and promoted the apoptosis of tumor cells via the downregulation of glycolytic enzyme expression and by reducing the mitochondrial membrane potential in ESCC. Bad, Caspase-3, Survivin, and Bcl-2 may be associated with blocking energy production and promoting apoptosis via miR-378a-3p in ESCC cells.

Correspondence to: Dr Hui Li, Central Laboratory of Xinjiang Medical University, Xinjiang Medical University, 393 Xinyi Road, Urumqi, Xinjiang 830011, P.R. China
E-mail: huihui922@126.com

Professor Huiwu Li, Medical Research Center, Yuebei People's Hospital, Shantou University, 133 South Huimin Road, Shaoguan, Guangdong 512025, P.R. China
E-mail: huiwuli1234@163.com

*Contributed equally

Key words: miR-378a-3p, glycolysis, esophageal squamous cell carcinoma, apoptosis

Introduction

Esophageal cancer is an aggressive malignancy of the digestive system with incidence rates of >450,000 cases worldwide, and 5-year-survival rates ranging from 15-25% (1). Data from the Chinese Cancer Center in 2022 demonstrated that esophageal cancer was the sixth most common malignant tumor and the fifth leading cause of cancer-related death (2). There are two major histological subtypes of esophageal cancer; namely, esophageal squamous cell carcinoma (ESCC) and adenocarcinoma (3). ESCC is the predominant histological classification of esophageal cancer in China with a 10-year survival rate of 14%, despite recent advances in therapeutics (4-6). Thus, further investigations into potential biomarkers for diagnosis and treatment, including oncogenes and tumor suppressor genes, are required.

MicroRNAs (miRNAs/miRs) are small RNAs that regulate the expression of complementary mRNAs (7). Numerous roles of miRNA have been identified in complex biological processes, such as metabolism (8), cancer (9), programmed cell death (10), cell proliferation, and differentiation (11). The results of a previous study demonstrated that there are a higher number of miRNAs in animals, and their regulatory impact is more pervasive than was previously suspected. Additionally, the same study showed that miRNAs can be used as diagnostic and prognostic markers for cancer (12). For example, miR-195

expression in ESCC is associated with a low survival rate (13). In colorectal cancer, the expression levels of miR-135b and miR-590-5p are associated with clinical stage and survival (7,14). miR-31-3p, -3676, -125a-5p, -100-5p, -125b-5p, -200a-5p, and miR-342 were significantly associated with the development of chemo- and radio-resistance in patients with locally advanced cervical cancer (15,16).

miR-378a is an intronic miRNA located in the peroxisome promoter-activated receptor γ activator 1-β gene and has been the focus of numerous studies (12,17-20). miR-378a-3p is the guide strand of miR-378a, and it is extensively associated with metabolism, while miR-378a-5p is regarded as the passenger strand (12). Notably, miR-378a-3p is the target gene of the oncogene Myc, which promotes tumor formation and angiogenesis in A549 adenocarcinoma cells (17). The results of further studies demonstrated that the expression of miR-378a-3p was reduced in ESCC tissues, which may lead to the overexpression of GLUT-1/SLC2A1 (21,22). Notably, the downregulation of miR-378a-3p induced decidual cell apoptosis, which contributed to early pregnancy loss (23). Therefore, the biological roles of miR-378a-3p in tumor cells remain contested. In addition, the association between functions, energy metabolism, and cell survival mechanisms in ESCC cells remains to be fully elucidated.

The energy metabolism of cancer cells, which exhibit increased metabolic requirements, is markedly different from healthy cells. In addition, cancer cells consume high quantities of glucose and produce lactic acid rather than catabolizing glucose through the tricarboxylic acid cycle. During this process, cancer cells generate higher levels of energy to further support their rapid proliferation (24). Genes associated with glycolysis, such as Aldolase A (ALDOA), Enolase 1 (ENO1), lactate dehydrogenase A (LDHA), phosphofructokinase L (PFKL), phosphoglycerate kinase 1 (PGK1), hexokinase-2 (HK2), 2,3-phosphoglyceraldehyde-3-phosphate dehydrogenation (GAPDH), and pyruvate kinase M2 (PKM2) participate in the energy metabolism of nucleosides, amino acids, and glucose, affect cell survival and apoptosis, and play a role in drug resistance and other biological mechanisms, to maintain the stability of tissue and the cellular environment (25,26).

The coding gene of Survivin, BIRC5, is located on human chromosome 17q25 and consists of three introns and four exons (27). Survivin is the smallest member of the inhibitor of apoptosis protein family. Wild-type Survivin is composed of 142 amino acids and often exists as a homodimer in the cytoplasm. Numerous previous studies have demonstrated that Survivin interacts with a variety of endogenous and exogenous apoptotic regulatory factors, such as Bad and Bcl-2, and significantly inhibits apoptosis via directly inhibiting the activities of Caspase-3 and Caspase-7, to block induced apoptosis (28-31).

In the present study, miR-378a-3p mimic and negative control were transfected into ECA-109 cells to detect and analyze the molecular regulatory process of miR-378a-3p. This interfered with its target genes, energy metabolism and the apoptosis of ESCC cells. The study will help us gain a deeper understanding of the regulatory mechanism of miR-378a-3p on tumor cells at the molecular biology level, and help us to understand the process of its intervention in tumor cells; it may also provide a novel theoretical basis for targeting miR-378a-3p as an interventional measure in the future.

Materials and methods

Cell culture. ESCC cell line ECA-109 was purchased from The BeNa Culture Collection (BNCC). The BNCC data showed that ECA-109 esophageal cancer cell line, established in 1973, originated from human esophageal middle squamous cell carcinoma tissue (ESCC). ECA-109 cells are considered one of the most representative models of ESCC (32-34). STR profiling was performed to confirm the identity of the cells. The cells were cultured in RPMI 1640 medium containing 10% FBS and 1% penicillin-streptomycin solution (penicillin 100 U/ml + streptomycin 100 mg/ml; all from Biological Industries). Cells were maintained in a humidified incubator at 37˚C supplied with 5% CO_2.

Determination of miR-378a-3p targets. First, the downstream target genes of miR-378a-3p in miRDB (https://mirdb.org) were screened. In view of its known interference in some energy metabolism related proteins, the 3' non-coding regions of all glucose metabolism-related gene mRNAs were compared. Due to the phenomenon of incomplete matching of miRNA sequences that interfere with the target protein translation process (8,9), if the 6-8 nt at the 5'end of miRNA was complementary to the target gene, and the basic principle of 'A' at the first nucleotide of the miRNA corresponding to the target gene (8,9), the gene was considered a target gene (Fig. 1A).

qPCR analysis. Total RNA was extracted from the cells using TRIzol® reagent (cat. no. 15596026; Thermo Fisher Scientific, Inc.). The extracted Total RNA was reverse transcribed into cDNA using the Mir-X miRNA first strand synthesis kit according to the manufacturer's instructions (cat. no. 638315; Clontech; Takara Bio USA, Inc.), and qPCR was performed using SYBR Green I Master (cat. no. 4887352001; Roche Diagnostics), with U6 as an inner control. A ightCycler 480 II (Roche Diagnostics) was used for the qPCR. The qPCR conditions were as follows: Pre-denaturation at 95˚C for 15 min, followed by 40 cycles of 10 sec of denaturation at 95˚C, annealing at 60˚C for 20 sec and extension at 72˚C for 20 sec. The fluorescence signals were collected at 72-95˚C after the reaction for melting curve analysis. The results were analyzed using a hyperbolic curve and the relative gene expression was determined. The forward primer sequences of miR-378a-3p were forward (F), 5'-ACTGGACTTGGAGTCAGAAGGC-3' and reverse (R), mRQ 3' primer in Mir-X miRNA First-Strand Synthesis Kit (cat. no. 638315; Clontech; Takara Bio USA Inc.). Primer sequences for U6 were F, 5'-GGAACGATACAGAGAAGATTAGC-3' and R, 5'-TGGAACGCTTCACGAATTTGCG-3'. The comparative Cq method was used to quantify gene levels using the formula: $^{\Delta}Cq=Cq_{miRNA}-Cq_{U6}$. $^{\Delta\Delta}Cq=\Delta Cq_{ApoE}-\Delta Cq_{WT}$. The relative quantification for miRNA was calculated as $2^{-\Delta\Delta Cq}$. Expression of miRNA was normalized by U6. The specific primers/sequences for amplifying miRNAs and mRNAs are listed in Table I.

Overexpression of miR-378a-3p. miRNA mimics and their negative control counterparts, miRNA-sponge or miRNA-shRNA expression plasmids were obtained, and the

Table I. Basic information on the synthesis and expression construction for miR-378a-3p.

miRNAs or gene clones	Sequence (5'-3')	Vector	Supplier
hsa-miR-378a-3p mimics	ACUGGACUUGGAGUCAGAAGGC		Shanghai GenePharma Co., Ltd.
mimic NC	UUCUCCGAACGUGUCACGUTT		Shanghai GenePharma Co., Ltd.
miR-378a-3p	GGATCCCCTTCTGACGACAGTCC	CMV-MCS-polyA-EF1A-zsGreen-sv40-puromycin	Shanghai Genechem Co., Ltd.
miRNA sponge	AGTCTTCCCTTCTGACGACAGTC CAGTCTTCCCTTCTGACGACAGT CCAGTCTTCCCTTCTGACGACAG TCCAGTCTTCCCTTCTGACGACA GTCCAGTCTTCCCTTCTGACGAC AGTCCAGTCTTCACCGGT		
miR-378a-3p shRNA-F	CCGGACTGGACTTGGAGTCAGA AGGCCTCGAGGCCTTCTGACTC CAAGTCCAGTTTTTTTG	LKD006 pLKD-Ubc-eGFP-U6-shRNA	OBiO Technology (Shanghai) Corp., Ltd.
miR-378a-3p shRNA-R	AATTCAAAAAAACTGGACTTGG AGTCAGAAGGCCTCGAGGCCTT CTGACTCCAAGTCCAGT	LKD006 pLKD-Ubc-eGFP-U6-shRNA	OBiO Technology (Shanghai) Corp., Ltd.
miR NC-F	CCGG TTCTCCGAACGTGTCACG TTTCAAGAGAACGTGACACGTT CGGAGAATTTTTTG	LKD006 pLKD-Ubc-eGFP-U6-shRNA-(NC)	OBiO Technology (Shanghai) Corp., Ltd.
miR NC-R	AATTCAAAAAATTCTCCGAACG TGTCACGT TCTCTTGAAACGTG ACACGTTCGGAGAA	LKD006 pLKD-Ubc-eGFP-U6-(NC)	OBiO Technology (Shanghai) Corp., Ltd.
ALDOA [NM_184041-3utr (mir378a-3p)-mut]	TCTAGATGTCAAGGAAAGTACA CTCCGAGCGGTCAGGCTGGGG CTGCTGCCAGCGAGTCCCTCTT CGTCTCTAACCACGCCTATTAAG CGGAGGTGTTCCCAGGCTTAAC CACACCAGAACGTCAAGTCCCC CTCCCACTCTTGAAGAGGAGGC CGCCTCCTCGGGGCTCCAGGCT GGCTTGCCCGCGCTCTTTCTTCC CTCGTGACAGTGGTGTGTGGTG TCGTCTCTAGA	GV272	Shanghai Genechem Co., Ltd.
ALDOA [NM_184041-3 utr (mir-378a-3p)]	TCTAGAGCTCTGCCCCTTCACCT AACAGCATAAGATAGGGCTAAC AGTTGGGGAGTATGGTTGTAACT GCTCATGTCTTAGGAGGCTTCAG CCTCAGCACTTTTAGGTCCAGAA CTCAAGGGGGGCAGAAGACCCC TGTGACAAAAACCCACTAACTAG CTCATGAGTGACATGAGCCAGGC AACATAATGGGTGTTTTATATGAG TAGATGTCTAGA	GV272	Shanghai Genechem Co., Ltd.
PKM2 [NM_002654 (mir-378a-3p)-mut]	TCTAGAGGGCTGAGGACGTGGA CCTCCGGGTGAACTTTGCCATGA ATGTTGGCAAGGCCCGAGGCTTC TTCAAGAAGGGAGATGTGGTCAT TGTGCTGACCGGATGTAGCCAGT GAGAAGGCGTACCCAACACCATG CGTGTTGTTCCTGTGCCGTGATGG ACCCCAGAGCCCCTCCTCCAGCC	GV272	Shanghai Genechem Co., Ltd.

Table I. Continued.

miRNAs or gene clones	Sequence (5'-3')	Vector	Supplier
	CCTGTCCCACCCCCTTCCCCCAGC		
	CCATCCATTAGGCCAGCATCTAGA		
PKM2	TCTAGAGGGCTGAGGACGTGGAC	GV272	Shanghai Genechem Co., Ltd.
[NM_002654	CTCCGGGTGAACTTTGCCATGAAT		
(mir-378a-3p)]	GTTGGCAAGGCCCGAGGCTTCTTC		
	AAGAAGGGAGATGTGGTCATTGTG		
	CTGACCGGATGGCGCCCTGGCTCC		
	GGCTTCACCAACACCATGCGTGTT		
	GTTCCTGTGCCGTGATGGACCCCA		
	GAGCCCCTCCTCCAGCCCCTGTCC		
	CACCCCCTTCCCCCAGCCCATCCAT		
	TAGGCCAGCATCTAGA		
SLC2A1	TCTAGACTCTGGTTCCTCTGTATAC	GV272	Shanghai Genechem Co., Ltd.
[NM_006516-3utr	TACTGCTTCATCTCTAAAGACAGC		
(mir378a-3p)-mut]	TCATCCTCCTCCTTCACCCCTGAAT		
	TTCCAGAGCACTTCATCTTATCCTG		
	CCTCAACCTGAACTTTTTCTGCCA		
	CTAGTCTGAATTTCATGAGAAGATG		
	CCGATTTGGTTCCTGTGGGTCCTCA		
	GCACTATTCAGTACAGTGCTTGATG		
	CACAGCAGGCACTCATCTAGA		
SLC2A1	TCTAGACTCTGGTTCCTCTGTATAC	GV272	Shanghai Genechem Co., Ltd.
[NM_006516-3utr	TACTGCTTCATCTCTAAAGACAGC		
(mir378a-3p)]	TCATCCTCCTCCTTCACCCCTGAAT		
	TTCCAGAGCACTTCATCTGCTCCTT		
	CATCACAAGTCCAGTTTTCTGCCA		
	CTAGTCTGAATTTCATGAGAAGATG		
	CCGATTTGGTTCCTGTGGGTCCTCA		
	GCACTATTCAGTACAGTGCTTGATG		
	CACAGCAGGCACTCATCTAGA		

miRNA/miR, microRNA; shRNA, short hairpin RNA; utr, untranslated region; NC, negative control; F, forward; R, reverse; ALDOA, aldolase A; PKM2, pyruvate kinase M2; SLC2A1, solute carrier family 2 member 1/glucose transporter protein 1.

information on their sequences and construction vectors are shown in Table I. Transient transfection with miRNA and DNA (expression plasmid) was performed using Lipofectamine™ 3000 (cat. no. L3000015; Invitrogen; Thermo Fisher Scientific, Inc.) in accordance with the manufacturer's protocols. Cells ($2x10^5$) were seeded into 6-well plates 1 day before transfection with 50 pmol miRNA mimics and negative control or 2.5 μg plasmid DNA using 5.0 μl Lipofectamine. After transient transfection (15 h), cells were washed with PBS (cat. no. C10010500BT; Thermo Fisher Scientific, Inc.) and used for experiments.

miR-378a-3p-shRNA overexpression and negative control plasmids (Table I) were transfected into cells during the logarithmic growth stage using electroporation (conditions: U, 280 V; C, 900 CF; R, 550 Ω) with Opti-MEM reduced serum medium (Gibco; Thermo Fisher Scientific, Inc.) with Gene Pulser XcellTM Electroporation System (Bio-Rad, USA).

Protein expression and cellular localization of TF-1 apoptosis-related gene-19 (TFAR19). Prior to cell inoculation, a cover glass was placed in each well of a 6-well plate. Cells ($1x10^5$) were inoculated on the cover glass to make cell slides. miR-378a-3p mimic RNAs were transfected into cells in the logarithmic growth stage using Lipofectamine 3000. After 15 h of transfection, the medium was discarded, and the cells were rinsed twice with PBS buffer. Subsequently, cells were fixed with 4% paraformaldehyde (cat. no. G0528; GBCBIO Technologies, Inc.) for 30 min at room temperature (22-25˚C), washed twice with PBS and sealed with blocking buffer for 1 h at room temperature.

Following blocking, cells were incubated overnight at 4˚C with the anti-TFAR19 primary antibody (1:300; cat. no. K107297P; Beijing Solarbio Science & Technology Co., Ltd.). Following primary incubation, cells were washed with PBS for 5 min, and subsequently incubated

with FITC-goat anti-rabbit secondary antibody (1:1,000; cat. no. A0562; Beyotime Institute of Biotechnology) for 1-2 h at room temperature. Cells were rinsed with PBS three times for 5 min each time, and stained with DAPI (Beyotime Institute of Biotechnology) in the dark for 3 min. Cells were rinsed again using PBS three times for 5 min each time. A drop of an anti-fluorescence quenching sealing agent was added to the slide and cells were subsequently observed using an inverted fluorescence microscope at x400 magnification (IX83; Olympus Corporation).

Western blotting. Following 24/48 h transfection, cells were collected and lysed at 4˚C for 30 min using RIPA lysate (Boster Biological Technology) supplemented with 1% protease inhibitor (Thermo Fisher Scientific, Inc.) and 1% phosphatase inhibitor (Thermo Fisher Scientific, Inc.). The supernatant was centrifuged (13,000 x g at 4˚C for 15 min) to obtain the total protein. Protein concentration was determined using a BCA Protein Assay kit (Thermo Fisher Scientific, Inc.). A total of 25 μg protein was loaded per lane on a 10% SDS-gel, resolved using SDS-PAGE, and transferred to PVDF membranes (Roche Diagnostics GmbH), which were subsequently blocked with TBS-Tween-20 (TBS-T) containing 5% skimmed milk at room temperature for 1 h. Following blocking, membranes were incubated overnight at 4˚C with the following primary antibodies against GLUT-1 (1:100,000; Abcam, cat. no. ab115730), ALDOA (1:1,000; Abcam, cat. no. ab252953), PKM2 (1:1,000; Cell Signaling Technology, Inc., cat. no. 4053T), H2AX (1:1,000; Cell Signaling Technology, Inc., cat. no. 7631S), p-H2AX (1:1,000; Cell Signaling Technology, Inc., cat. no. 9718S), Caspase-3 (1:1,000; Cell Signaling Technology, Inc., cat. no. 9662S), cleaved Caspase-3 (1:1,000; Abcam, cat. no. AB32042), Bad (1:1,000; Cell Signaling Technology, Inc., cat. no. 9268S), Survivin (1:1,000; Cell Signaling Technology, Inc., cat. no. 2808S), Bcl-2 (1:1,000; Cell Signaling Technology, Inc., cat. no. 15071S), β-actin (1:1,000; Cell Signaling Technology, Inc., cat. no. 3700S), and TFAR19 (1:1,000; Beijing Solarbio Science & Technology Co., Ltd., cat. no. K107297P). The following secondary antibodies were used: anti-mouse antibody (Cell Signaling Technology, Inc., cat. no. 7076S, Lot#35, 1:4,000) anti-rabbit antibody (Cell Signaling Technology, Inc., cat. no. 7074S, Lot#30, 1:3,000). Following primary incubation, membranes were incubated at room temperature for 1 h with the secondary antibody, anti-mouse/rabbit HRP-conjugated antibodies. Following washing with TBS-T, signals were visualized using an enhanced chemiluminescence detection reagent (Thermo Fisher Scientific, Inc.). β-actin was used as the loading control. Image J version 1.53 was used for densitometry (National Institutes of Health).

Flow cytometry. A FITC Annexin V Apoptosis Detection kit (BD Biosciences) was used to detect the apoptosis of cells. Transfected cells in each group were collected, washed twice with pre-cooled PBS, and suspended in 1X binding buffer. A total of 5 μl FITC and 5 μl PI were added for incubation for 15 min at 25˚C. Subsequently, 400 μl 1X binding buffer was added to each tube and analyzed using flow cytometry (FACSAria II) with BD FACSDiva software (version 8.0.2) (Becton, Dickinson and Company) within 1 h.

ELISA. Cells in the control, NC and miR378-mimics groups transfected for 24 or 48 h were collected and washed with pre-cooled PBS three times. A total of 250 μl NP40 lysate was added to cells for 30 min until cells were fully lysed, and the supernatant was collected. The ELISA kits (Human ALDOA ELISA Kit, cat. no. E-EL-H0309-96T, Lot# BRZUPTIBFG; Human GLUT-1 ELISA Kit, cat. no. E-EL-H1822-96T, Lot# 3MIHWZGF38; Human PKM2 ELISA Kit, cat. no. E-EL-H1089-96T, Lot# IUNGNXEV9W; Elabscience Biotechnology, Inc.) were used according to the manufacturer's instructions. The optical density of each well was measured using a microplate reader at a wavelength of 450 nm. The concentration of total protein was considered the level of the enzyme.

Detection of the dual-luciferase reporter assay. A Dual Luciferase Reporter Gene Assay kit (Beijing Solarbio Science & Technology Co., Ltd.) was used to assess the target genes of miR-378a-3p (Table I). Cells were co-transfected with the wild-type/mutant plasmid DNA of the respective firefly luciferase target genes + *Renilla* luciferase plasmid DNA ± miR-378a-3p plasmid DNA, and cultured for 24/48 h. Lysate was collected after cells (200 μl lysate/1x10^6 cells) were fully lysed at 4˚C for 5 min. A total of 20 μl cell lysate was added to 100 μl 1X firefly/*Renilla* luciferase reaction solution, and luciferase activity was detected. Firefly luciferase activity/*Renilla* luciferase activity was measured as luciferase reporter gene activity.

ATP synthesis inhibition. Oligomycin (concentration, 200 nM) was used in ECA109 cells in the logarithmic growth phase for 12 or 24 h to inhibit ATP synthetase and decrease the ATP content in cells.

ATP detection. ATP Detection kit (Beijing Solarbio Science & Technology Co., Ltd.) was used to determine the ATP content of cells. Cells were suspended with ATP extract (1 ml/5x10^6 cells) and lysed using ultrasonication. Chloroform was mixed with 100 μl supernatant or the control and 900 μl ATP detection working solution, and the absorbance was measured at 10 sec and 3 min 10 sec with a wavelength of 340 nm (recorded as A1 and A2, respectively), using an ultraviolet spectrophotometer. DA=A2-A1; DA/(DA standard/C standard) x V extract/5 as ATP content (μmol/10^6 cells).

Detection of mitochondrial membrane potential. An enhanced mitochondrial membrane potential detection kit (JC-1) (cat. no. C2003S, Beyotime Institute of Biotechnology) was used to determine the mitochondrial membrane potential. For each well of a 6-well plate, the media was removed, cells were washed with PBS once, 1 ml cell culture medium was added, and 1 ml JC-1 dye working solution was added and mixed thoroughly. Next cells were incubated for 20 min. After incubation, the supernatant was aspirated, and cells were washed twice with JC-1 dye buffer. and 2 ml cell culture medium was added. Cells were observed using an inverted fluorescence microscope at x100 and x400 magnification (IX83; Olympus Corporation). When detecting JC-1 monomers, the excitation light wavelength was set to 490 nm and the emission light wavelength was set to 530 nm; when observing the JC-1 polymer, the excitation light wavelength was set to 525 nm and the emission light wavelength was set to 590 nm.

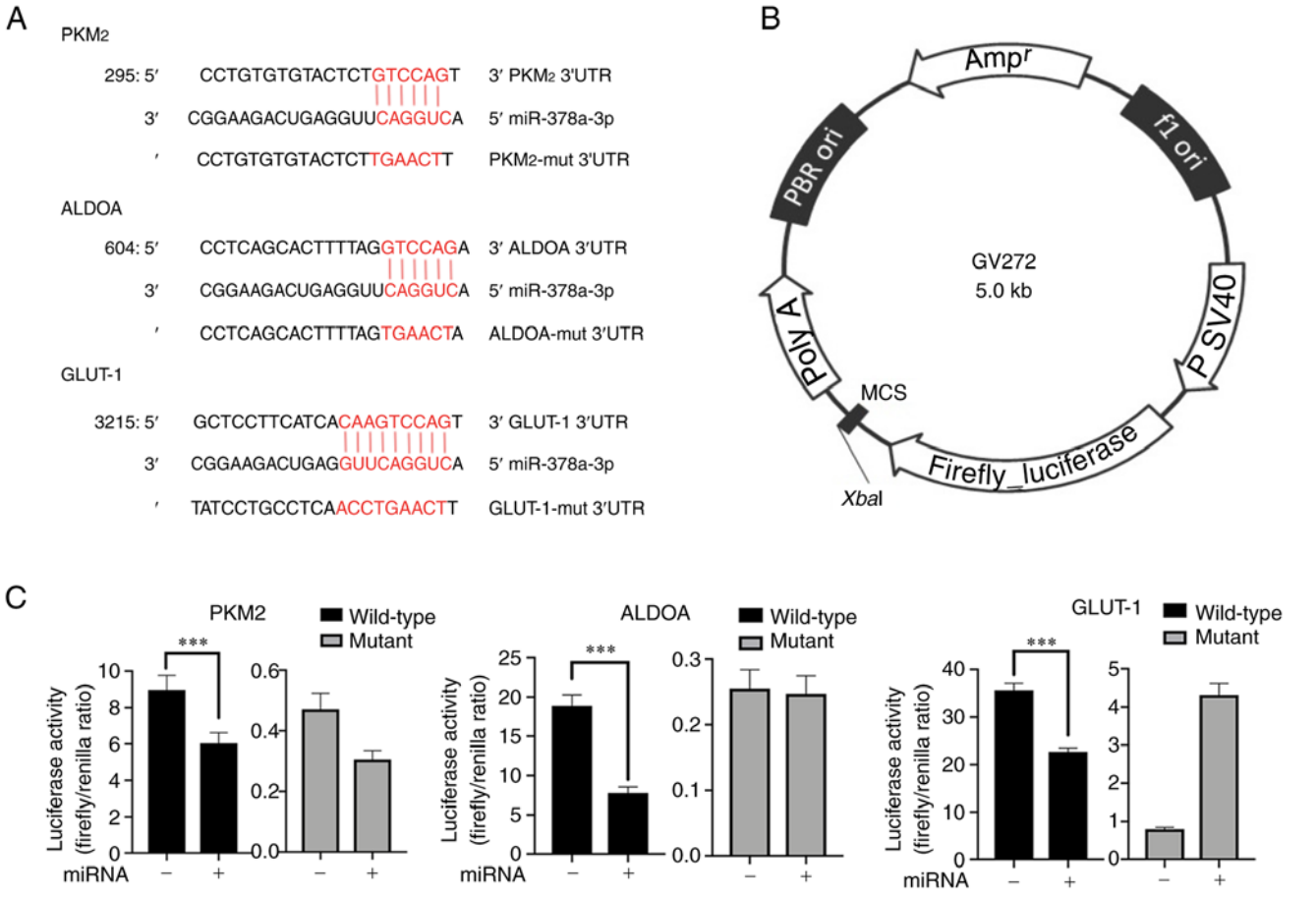

Figure 1. PKM2, ALDOA, and GLUT-1 are target genes of miR-378a-3p. (A) The matching sites between miR-378a-3p and wild-type/mutant genes of PKM2, ALDOA, and GLUT-1. (B) Construction of the dual-luciferase reporter vector. (C) The activity of firefly luciferase reporter genes PKM2, ALDOA, and GLUT-1 was suppressed by miR-378a-3p in ECA-109 cells. ***P<0.001. miR/miRNA, microRNA; mut, mutant; PBR, a man-made constructed plasmid DNA; ori, the replication origin of plasmid; amp^r, antiampicillin-resistance gene.

Statistical analysis. All data were analyzed in GraphPad Prism (version, 8.0.0, GraphPad Software, Inc.]. All quantitative data are presented as the mean ± standard deviation. A one-way ANOVA followed by Tukey's post hoc test was used to analyze the difference between multiple groups. P<0.05 was considered to indicate a statistically significant difference. All the experiments were performed at least three times.

Results

Baseline miR-378a-3p expression levels in ECA-109 cells. A miR-378a-3p-sponge overexpression vector was used to establish the baseline miR-378-3p expression levels (Table I). The results showed that the expression of miR-378a-3p was very low in ECA-109 cells (Fig. S1A and B), indicating that its expression as a tumor suppressor gene was suppressed. At low levels, miR-378a-3p had limited effect on the normal biological activity of ECA-109 cells as the miR-378a-3p-sponge had limited effect on GLUT-1, ALDOA, and PKM2 protein levels in ECA-109 cells (Fig. S1C and D).

ALDOA/GLUT-1/PKM2 are target genes of miR-378a-3p. To identify the target genes of miR-378a-3p, a dual-luciferase reporter assay was performed using a GV272 vector containing the wild-type or mutant miR-378a-3p-binding sequences in the 3'-untranslated region (UTR) of ALDOA, GLUT-1, PKM2, LDHA, and GAPDH. miR-378a-3p mimic and the reporter vector were co-transfected into ECA-109 cells. The results of the present study indicated that miR-378-3p markedly suppressed the dual-luciferase activity of key enzymes of glycolysis, including ALDOA, GLUT-1, and PKM2 (Fig. 1).

Expression levels of glycolysis-related enzymes are downregulated by miR-378a-3p mimic transfection. Based on the aforementioned findings that miR-378a-3p directly targeted glycolytic enzymes, the effects of miR-378a-3p on the glycolysis pathway were determined. Following miR-378a-3p transfection, the association between miR-378a-3p and energy metabolism was assessed. The major enzymes of the glycolysis pathway were detected using western blotting and ELISA. Protein expression levels and enzyme activities of PKM2, ALDOA, and GLUT-1 were inhibited between 24 and 48 h following transfection of miR-378a-3p (Fig. 2).

Survivin expression levels are downregulated, while Bad and Caspase-3 expression levels are upregulated by miR-378a-3p. To investigate the potential mechanism by which miR-378a-3p affected the apoptosis of ECA-109 cells at the protein level, protein expression levels of Bad, Caspase-3, and Survivin were investigated. The results showed that in the group of

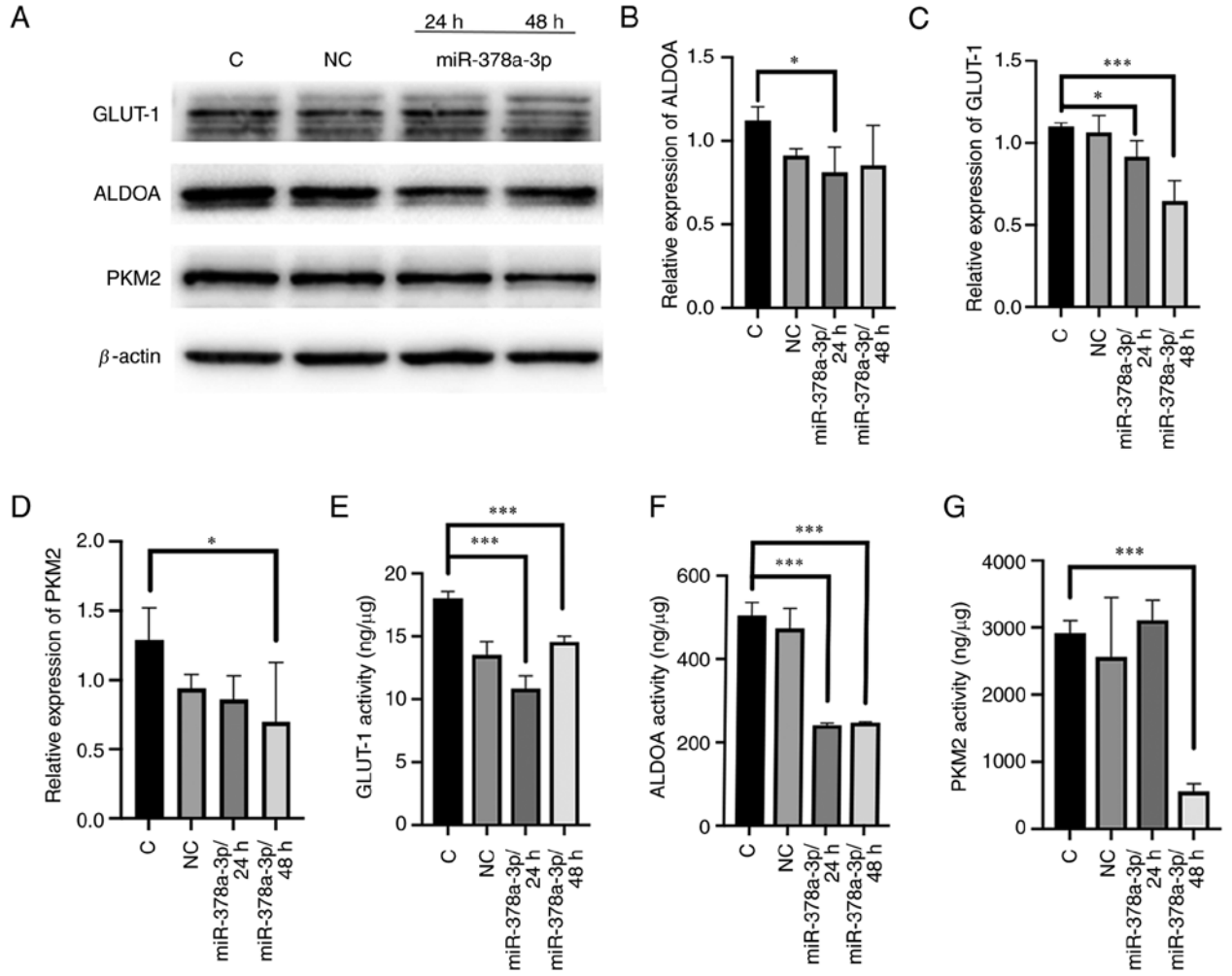

Figure 2. miR-378a-3p inhibits the expression of glycolysis-related enzymes. (A) Representative western blots of glycolysis-related enzymes in cells transfected with miR-378a-3p. Relative protein expression levels of (B) ALDOA, (C) GLUT-1 and (D) PKM2 were downregulated by miR-378a-3p. Enzyme levels of (E) GLUT-1, (F) ALDOA and (G) PKM2 were suppressed by transfected miR-378a-3p. *P<0.05, ***P<0.001. NC, negative control; C, control; miR, microRNA; GLUT-1, glucose transport 1; ALDOA, aldolase A; PKM2, pyruvate kinase M2.

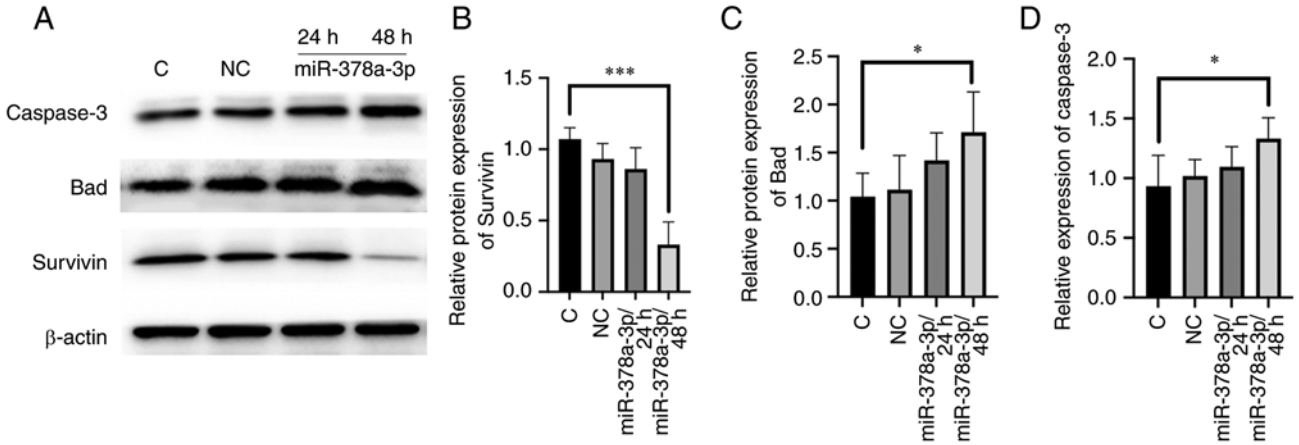

Figure 3. miR-378a-3p inhibits the expression of apoptosis inhibitor protein and promotes the expression of apoptosis-related proteins. (A) Representative western blot of apoptosis-related proteins (Bad, Caspase-3 and Survivin). Relative protein expression levels of (B) Survivin were decreased, and those of (C) Bad and (D) Caspase-3 were increased by transfection with miR-378a-3p mimics. *P<0.05, ***P<0.001. NC, negative control; C, control; miR, microRNA; GLUT-1, glucose transport 1; ALDOA, aldolase A; PKM2, pyruvate kinase M2.

transfected with miR-378a-3p mimics, Survivin expression (an apoptosis inhibitor protein) was markedly decreased, while Caspase-3 and Bad expression (apoptosis-related proteins) were increased (Fig. 3). Cleaved caspase-3 expression was

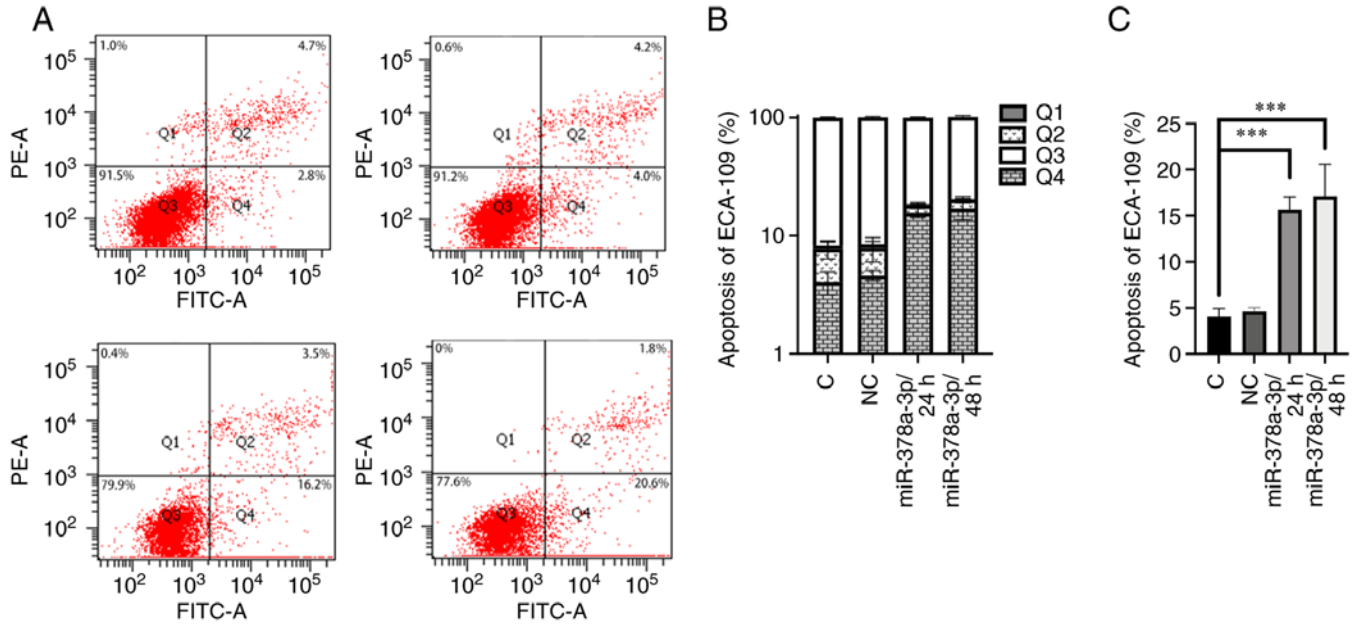

Figure 4. miR-378a-3p promotes apoptosis in ECA-109 cells. (A-C) Compared with the control or miR-NC group, the ratio of cell apoptosis was markedly increased, particularly in the stage (Q4). ***P<0.001. NC, negative control; C, control; miR, microRNA.

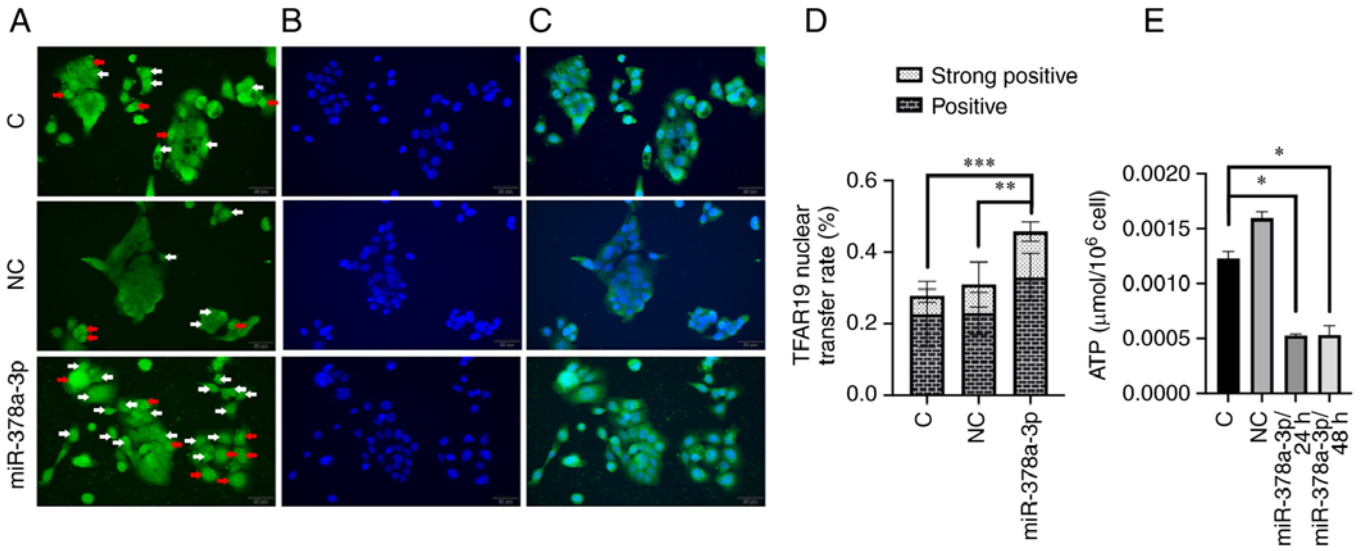

Figure 5. TFAR19 nuclear translocation is observed in the group transfected with miR-378a-3p mimics. (A-D) Compared with the control or miR-negative control, a strong positive reaction of FITC-TFAR19 staining was observed in the miR-378a-3p mimics transfection group. Red arrow, TFAR19 levels were significantly higher in the nucleus than in the cytoplasm, defined as strongly positive. White arrow, TFAR19 levels were higher in the nucleus than in the cytoplasm, defined as positive. In other cells, TFAR19 levels were equivalent in the nucleus and cytoplasm, or lower in the nucleus than in the cytoplasm, defined as negative. (B) DAPI staining of each group. (C) FITC-TFAR19 and DAPI overlay images. (E) ATP content of cells was significantly decreased in the group transfected with miR-378a-3p mimics. *P<0.05, **P<0.01, ***P<0.001. NC, negative control; C, control; miR, microRNA; TF-1 apoptosis-related gene-19.

increased (Fig. S2). To confirm that there was no DNA damage involved in the early stage of apoptosis, histone variant H2AX phosphorylation was detected by western blotting, and it was shown that their protein levels were not increased following miR-378a-3p overexpression (Fig. S2).

Transfected with miR-378a-3p mimics promotes cell apoptosis. A cell apoptosis assay was performed to determine the biological function of miR-378a-3p. ECA-109 cells were transfected with miR-378a-3p mimics and negative control RNAs, and the cells were collected 24 and 48 h later. The results showed that in the miR-378a-3p mimic treatment group, the number of apoptotic cells in the early stage was significantly higher than that in the control or miR-NC negative control group (Fig. 4).

TFAR19 nuclear translocation is enhanced by miR-378a-3p. TFAR19, also known as programmed cell death 5 (PDCD5), cellular localization analysis was performed to verify the role of miR-378a-3p in promoting cell apoptosis. There was notable TFAR19 nuclear translocation in the miR-378a-3p mimics transfected group (Fig. 5A-D).

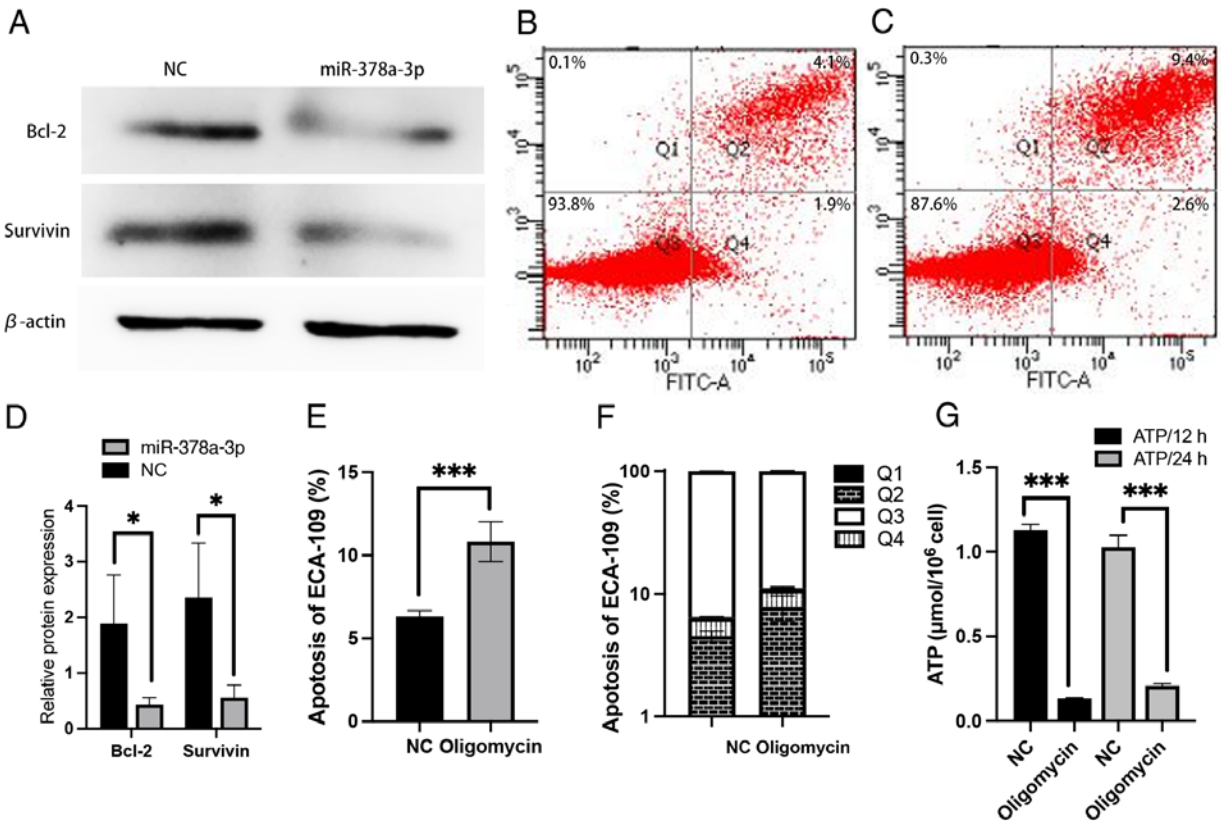

Figure 6. Oligomycin promotes cell apoptosis by blocking ATP generation and inhibiting the expression levels of apoptosis inhibitor proteins. (A and D) Bcl-2 and Survivin were suppressed following treatment with oligomycin. (B, C, E, F) Compared with the control group, the ratio of cell apoptosis was increased following treatment with oligomycin. (G) ATP content of cells was markedly decreased following treatment with oligomycin for 12 and 24 h. *P<0.05, ***P<0.001. NC, negative control; miR, microRNA.

Energy metabolism is suppressed by miR-378a-3p. To further clarify the impact of miR-378a-3p on cancer cell apoptosis, the ATP content was determined. Following transfection with miR-378a-3p mimics or negative control miRNA for 24/48 h, it was shown that miR-378a-3p blocked energy metabolism, resulting in a decrease in ATP in the miR-378a-3p group (Fig. 5E). The mitochondrial membrane potential was also significantly decreased (Figs. S3 and S4).

Oligomycin leads to ATP loss, reduced expression of Survivin and Bcl-2, and increased cell apoptosis. To further verify the association between energy metabolism and apoptosis, oligomycin was used to inhibit ATP synthase. The results of the present study demonstrated that the ATP content, and the protein expression levels of Survivin and Bcl-2 were significantly decreased following treatment with oligomycin. These results indicated that inhibition of ATP synthesis may lead to apoptosis via alterations in the expression of Survivin and Bcl-2 (Fig. 6).

Discussion

miRNAs have been widely studied due to their anti-oncogenic functions. miRNAs are small non-coding RNA molecules that bind target mRNAs via complementary sequences in the 3'-UTR to inhibit their expression. Low expression of miR-378a-3p is closely associated with an unfavorable prognosis, which has been demonstrated in numerous different types of cancer cells, such as pancreatic cancer (35), ovarian cancer (36), and ESCC tissues (21). However, the results of previous studies involving the biological functions of miR-378 in tumor cells remain contested. Gao *et al* (37) demonstrated that miR-378 was involved in the inhibition of apoptosis of tumor cells by impacting the activity of p53 and Caspase-3 in lung cancer cells (37). In gastric cancer tissues, Yang *et al* (38) demonstrated that miR-378 may be a tumor suppressor gene, promoting cell apoptosis through BMP2 (38). Cui *et al* (39) also showed that miR-378a-3p/5p inhibited the tumor migration and invasion of oral squamous carcinoma cells through decreasing KLK4 expression (39). The miR-378a-3p/GLUT-1 regulatory model may be a novel therapeutic target in the metabolic remodeling of patients with ESCC (22). Survivin is an important inhibitor of apoptosis and plays a role in the survival of tumor cells (31). Survivin supports the survival of tumor cells by inhibiting the endogenous apoptosis pathway and the activity of apoptosis-related factors (30). In addition, Survivin is associated with the Akt/mTOR and NF-κB signaling pathways, which have previously been shown to be active in different cancer cell lines (40-47). Moreover, the results of a previous study demonstrated the positive cyclic regulation of Survivin and NF-κB (48). However, there are no studies assessing the association between miR-378a-3p and Survivin to the best of our knowledge. Thus, further investigations into the regulatory mechanisms of energy metabolism and apoptosis in ESCC cells may improve the current understanding of its

regulation, and provide a novel experimental basis for determining the biological role and significance of miR-378a-3p in ESCC cells.

The glycolytic bioenergetics pathway is an important source of energy in tumor cells. The primary metabolic enzymes in this pathway include GLUT-1, HK2, PFKL, ALDOA, GAPDH, PGK1, ENO1, PKM2, and LDHA. Eichner *et al* (49) determined that miR-378a-3p decreased HK2 and LDHA expression, which may enhance oxidative phosphorylation, and suppress cell growth and tumorigenicity. Wang *et al* (50) also showed that miR-378a-3p repressed GLUT-1 expression by directly targeting its 3'UTR, and thus accelerated oral squamous cell carcinoma metastasis.

In the present study, it was first confirmed that ALDOA and PKM2 were the direct downstream target genes of miR-378a-3p. The results of the present study demonstrated that miR-378a-3p may block energy production in tumor cells by inhibiting the protein expression levels of GLUT-1, ALDOA, and PKM2. Following miR-378a-3p overexpression, ATP content, and mitochondrial membrane potential were reduced and apoptosis was promoted via Survivin, Bcl-2, Bad, and Caspase-3. Moreover, to determine the association between cell energy metabolism and apoptosis, an inhibitor of ATP synthesis, oligomycin, was used to treat cells. The results of the present study demonstrated that the levels of apoptosis inhibitory proteins (Survivin and Bcl-2) were reduced, and apoptosis was increased following treatment; thus, confirming that miR-378a-3p may induce apoptosis through the intervention of cell energy metabolism. TFAR19 was initially identified as a widely expressed apoptosis-accelerating protein. TFAR19 rapidly translocates from the cytoplasm to the nucleus in the early stage of apoptosis (30,51). The results of the present study demonstrated that TFAR19 nuclear translocation was significant in the miR-378a-3p transfection group. Moreover, the results of the present study demonstrated that miR-378a-3p promoted apoptosis of tumor cells was mediated by an endogenous apoptosis mechanism related to the impairment of mitochondrial membrane potential, particularly in the early stage. Survivin, Bcl-2, Bad, and Caspase-3 are common proteins in the apoptotic pathway. Notably, alterations in the expression levels of Survivin, Bcl-2, Bad, and Caspase-3 in the miR-378a-3p overexpression group demonstrated that the mode of cell death induced by miR-378a-3p was apoptosis. These results indicated that miR-378a-3p promotes the apoptosis of tumor cells by increasing the expression and the activity of Bad and Caspase-3, and reducing the expression of Survivin and Bcl-2. The results demonstrating the energy metabolism of ESCC cells provide a novel experimental basis to further understand the association between energy metabolism and apoptosis. Notably, the results of the present study are consistent with those of previous studies, demonstrating the decline of metabolism, including the reduction of glycolysis, ATP levels, and protein production, and the triggering of the apoptosis pathway (49,50). Compared with previous studies, it is hypothesized that miR-378a-3p may promote apoptosis through interfering with cell energy metabolism in ESCC cells (16,30,32).

As energy metabolism is vital for the survival of tumor cells, further investigations into the specific molecular mechanism of miR-378a-3p in the regulation of enzymes associated with energy metabolism are required.

The present study is limited, as the mechanism by which miR-378a-3p inhibited the enzyme activity of HK2 and LDHA in ECA-109 cells remains to be fully elucidated. Thus, whether miR-378a-3p induced cell apoptosis via Survivin and the Akt/mTOR/NF-κB signaling pathway requires further investigation. Additionally, the influence of miR-378a-3p on cell migration, invasion, and proliferation should be determined.

In conclusion, the results of the present study revealed a novel association between miR-378a-3p, glycolysis, and apoptosis. Specifically, miR-378a-3p may block energy production and promote the apoptosis of tumor cells by downregulating glycolytic enzyme expression in ECA-109 cells. miR-378a-3p inhibits ATP synthase, increases the expression levels and activity of Bad and Caspase-3, and decreases the expression levels of Survivin and Bcl-2. These results provide novel evidence demonstrating that miR-378a-3p is a tumor suppressor gene. In addition, the results of the present study demonstrated that Survivin, Bad, and Bcl-2 may be associated with the miR-378a-3p-induced inhibition of energy production, and the miR-378a-3p-induced promotion of apoptosis. The anti-tumor effect of miR-378a-3p may provide a novel treatment option for the management of ESCC.

Acknowledgements

Not applicable.

Funding

This study was supported by funding the National Nature Science Foundation of China (grant nos. 81460359 and 81460419).

Availability of data and materials

The datasets used and/or analyzed during the present study are available from the corresponding author on reasonable request.

Authors' contributions

HL and HWL conceived and designed the experiments. YQ, SX, YJD, and LTH performed the experiments. YQ, YJZ and GPZ analyzed the data. YQ, YJZ and HWL confirm the authenticity of all the raw data. All authors reviewed and approved the final manuscript.

Ethics approval and consent to participate

Not applicable.

Patient consent for publication

Not applicable.

Competing interests

The authors declare that they have no competing interests.

References

1. Pennathur A, Gibson MK, Jobe BA and Luketich JD: Oesophageal carcinoma. Lancet 381: 400-412, 2013.
2. Zheng R, Zhang S, Zeng H, Wang S, Sun K, Sun R, Li L, Wei W and Wei J: Cancer incidence and mortality in China, 2016. J National Cancer Center 2: 1-9, 2022.
3. Kamangar F, Dores GM and Anderson WF: Patterns of cancer incidence, mortality, and prevalence across five continents: Defining priorities to reduce cancer disparities in different geographic regions of the world. J Clin Oncol 24: 2137-2150, 2006.
4. Guo P, Huang ZL, Yu P and Li K: Trends in cancer mortality in China: An update. Ann Oncol 23: 2755-2762, 2012.
5. Dubecz A, Gall I, Solymosi N, Schweigert M, Peters JH, Feith M and Stein HJ: Temporal trends in long-term survival and cure rates in esophageal cancer: A SEER database analysis. J Thorac Oncol 7: 443-447, 2012.
6. Ohashi S, Miyamoto S, Kikuchi O, Goto T, Amanuma Y and Muto M: Recent advances from basic and clinical studies of esophageal squamous cell carcinoma. Gastroenterology 149: 1700-1715, 2015.
7. Ambros V: The functions of animal microRNAs. Nature 431: 350-355, 2004.
8. Rottiers V and Naar AM: MicroRNAs in metabolism and metabolic disorders. Nat Rev Mol Cell Biol 13: 239-250, 2012.
9. Peng Y and Croce CM: The role of MicroRNAs in human cancer. Signal Transduct Target Ther 1: 15004, 2016.
10. Su Z, Yang Z, Xu Y, Chen Y and Yu QJO: MicroRNAs in apoptosis, autophagy and necroptosis. Oncotarget 6: 8474-8490, 2015.
11. Ivey KN and Srivastava D: MicroRNAs as regulators of differentiation and cell fate decisions. Cell Stem Cell 7: 36-41, 2010.
12. Machado IF, Teodoro JS, Palmeira CM and Rolo AP: miR-378a: A new emerging microRNA in metabolism. Cell Mol Life Sci 77: 1947-1958, 2020.
13. Liu B, Qu J, Xu F, Guo Y, Wang Y, Yu H and Qian B: MiR-195 suppresses non-small cell lung cancer by targeting CHEK1. Oncotarget 6: 9445-9456, 2015.
14. Valeri N, Braconi C, Gasparini P, Murgia C, Lampis A, Paulus-Hock V, Hart JR, Ueno L, Grivennikov SI, Lovat F, *et al*: MicroRNA-135b promotes cancer progression by acting as a downstream effector of oncogenic pathways in colon cancer. Cancer Cell 25: 469-483, 2014.
15. Pedroza-Torres A, Campos-Parra AD, Millan-Catalan O, Loissell-Baltazar YA, Zamudio-Meza H, Cantú de León D, Montalvo-Esquivel G, Isla-Ortiz D, Herrera LA, Ángeles-Zaragoza Ó, *et al*: MicroRNA-125 modulates radioresistance through targeting p21 in cervical cancer. Oncol Rep 39: 1532-1540, 2018.
16. Pedroza-Torres A, Fernández-Retana J, Peralta-Zaragoza O, Jacobo-Herrera N, Cantú de Leon D, Cerna-Cortés JF, Lopez-Camarillo C and Pérez-Plasencia C: A microRNA expression signature for clinical response in locally advanced cervical cancer. Gynecol Oncol 142: 557-565, 2016.
17. Chen LT, Xu SD, Xu H, Zhang JF, Ning JF and Wang SF: MicroRNA-378 is associated with non-small cell lung cancer brain metastasis by promoting cell migration, invasion and tumor angiogenesis. Med Oncol 29: 1673-1680, 2012.
18. Qin Y, Liang R, Lu P, Lai L and Zhu X: Depicting the Implication of miR-378a in Cancers. Technol Cancer Res Treat 21: 15330338221134385, 2022.
19. Krist B, Florczyk U, Pietraszek-Gremplewicz K, Józkowicz A and Dulak J: The role of miR-378a in metabolism, angiogenesis, and muscle biology. Int J Endocrinol 2015: 281756, 2015.
20. Wang Y and Du J: miR-378a-3p regulates glioma cell chemosensitivity to cisplatin through IGF1R. Open Life Sci 16: 1175-1181, 2021.
21. Ding N, Sun X, Wang T, Huang L, Wen J and Zhou Y: miR-378a-3p exerts tumor suppressive function on the tumorigenesis of esophageal squamous cell carcinoma by targeting Rab10. Int J Mol Med 42: 381-391, 2018.
22. Liu H, Zhang Q, Song Y, Hao Y, Cui Y, Zhang X, Zhang X, Qin Y, Zhu G, Wang F, *et al*: Long non-coding RNA SLC2A1-AS1 induced by GLI3 promotes aerobic glycolysis and progression in esophageal squamous cell carcinoma by sponging miR-378a-3p to enhance GLUT-1 expression. J Exp Clin Cancer Res 40: 287, 2021.
23. Hong L, Yu T, Xu H, Hou N, Cheng Q, Lai L, Wang Q, Sheng J and Huang H: Down-regulation of miR-378a-3p induces decidual cell apoptosis: A possible mechanism for early pregnancy loss. Hum Reprod 33: 11-22, 2018.
24. Vander Heiden MG, Cantley LC and Thompson CB: Understanding the Warburg effect: The metabolic requirements of cell proliferation. Science 324: 1029-1033, 2009.
25. Hong X, Zhong L, Xie Y, Zheng K, Pang J, Li Y, Yang Y, Xu X, Mi P, Cao H, *et al*: Matrine Reverses the Warburg effect and suppresses colon cancer cell growth via negatively regulating HIF-1α. Front Pharmacol 10: 1437, 2019.
26. Tirpe AA, Gulei D, Ciortea SM, Crivii C and Berindan-Neagoe I: Hypoxia: Overview on Hypoxia-Mediated mechanisms with a focus on the role of HIF genes. Int J Mol Sci 20: 6140, 2019.
27. Comelli M, Di Pancrazio F and Mavelli I: Apoptosis is induced by decline of mitochondrial ATP synthesis in erythroleukemia cells. Free Radic Biol Med 34: 1190-1199, 2003.
28. Marzieh A, Saeed T, Elina K, Omid V, Mortaza TA, Mahshid T and Amir S: Caspase-3: Structure, function, and biotechnological aspects. Biotechnol Appl Biochem 69: 1633-1645, 2022.
29. Altieri DC: Survivin-The inconvenient IAP. Semin Cell Dev Biol 39: 91-96, 2015.
30. Budhidarmo R and Day CL: IAPs: Modular regulators of cell signalling. Semin Cell Dev Biol 39: 80-90, 2015.
31. Chu SF, Zhang Z, Zhang W, Zhang MJ, Gao Y, Han N, Zuo W, Huang HY and Chen NH: Upregulating the expression of Survivin-HBXIP complex contributes to the protective role of IMM-H004 in transient global cerebral Ischemia/Reperfusion. Mol Neurobiol 54: 524-540, 2017.
32. Dai L, Li JL, Liang XQ, Li L, Feng Y, Liu HZ, Wei WE, Ning SF and Zhang LT: Flowers of Camellia nitidissima cause growth inhibition, cell-cycle dysregulation and apoptosis in a human esophageal squamous cell carcinoma cell line. Mol Med Rep 14: 1117-1122, 2016.
33. Zhang C, Ma Q, Shi Y, Li X, Wang M, Wang J, Ge J, Chen Z, Wang Z and Jiang H: A novel 5-fluorouracil-resistant human esophageal squamous cell carcinoma cell line Eca-109/5-FU with significant drug resistance-related characteristics. Oncol Rep 37: 2942-2954, 2017.
34. Yao J, Shen X, Li H, Xu J, Shao S, Huang JX and Lin M: LncRNA-ECM is overexpressed in esophageal squamous cell carcinoma and promotes tumor metastasis. Oncol Lett 16: 3935-3942, 2018.
35. Liu L, Han S, Xiao X, An X, Gladkich J, Hinz U, Hillmer S, Hoppe-Tichy T, Xu Y, Schaefer M, *et al*: Glucocorticoid-induced microRNA-378 signaling mediates the progression of pancreatic cancer by enhancing autophagy. Cell Death Dis 13: 1052. 2022.
36. Xu ZH, Yao TZ and Liu W: miR-378a-3p sensitizes ovarian cancer cells to cisplatin through targeting MAPK1/GRB2. Biomed Pharmacother 107: 1410-1417, 2018.
37. Gao S, Yu Y, Liu L, Meng J and Li G: Circular RNA hsa_circ_0007059 restrains proliferation and epithelial-mesenchymal transition in lung cancer cells via inhibiting microRNA-378. Life Scis 233: 116692, 2019.
38. Yang YJ, Luo S and Wang LS: Effects of microRNA-378 on epithelial-mesenchymal transition, migration, invasion and prognosis in gastric carcinoma by targeting BMP2. Eur Rev Med Pharmacol Sci 23: 5176-5186, 2019.
39. Cui Z, Sun S, Liu Q, Zhou X, Gao S, Peng P and Li Q: MicroRNA-378-3p/5p suppresses the migration and invasiveness of oral squamous carcinoma cells by inhibiting KLK4 expression. Biochem Cell Biol 98: 154-163, 2020.
40. Fu JH, Yang S, Nan CJ, Zhou CC, Lu DQ, Li S and Mu HQ: MiR-182 affects renal cancer cell proliferation, apoptosis, and invasion by regulating PI3K/AKT/mTOR signaling pathway. Eur Rev Med Pharmacol Sci 22: 351-357, 2018.
41. Ou DL, Lee BS, Lin LI, Liou JY, Liao SC, Hsu C and Cheng AL: Vertical blockade of the IGFR-PI3K/Akt/mTOR pathway for the treatment of hepatocellular carcinoma: The role of survivin. Mol Cancer 13: 2, 2014.
42. Meng Y, Lin ZM, Ge N, Zhang DL, Huang J and Kong F: Ursolic acid induces apoptosis of prostate cancer cells via the PI3K/Akt/mTOR pathway. Am J Chin Med 43: 1471-1486, 2015.
43. Khwairakpam AD, Monisha J, Roy NK, Bordoloi D, Padmavathi G, Banik K, Khatoon E and Kunnumakkara AB: Vietnamese coriander inhibits cell proliferation, survival and migration via suppression of Akt/mTOR pathway in oral squamous cell carcinoma. J Basic Clin Physiol Pharmacol: 31, 2019 doi: 10.1515/jbcpp-2019-0162.
44. Guo RH, Wang TS, Shen H, Ge HM, Sun J, Huang ZH and Shu YQ: Involvement of mTOR and survivin inhibition in tamoxifen-induced apoptosis in human hepatoblastoma cell line HepG2. Biomed Pharmacother 64: 249-253, 2010.

45. Li W, Du D and Li Y: Id-1 promotes reendothelialization in the early phase after vascular injury through activation of NFkB/survivin signaling pathway. Drug Des Devel Ther 13: 3799-3811, 2019.
46. Fukayama M, Hino R and Uozaki H: Epstein-Barr virus and gastric carcinoma: Virus-host interactions leading to carcinoma. Cancer Sci 99: 1726-1733, 2008.
47. Jeyasuria P, Subedi K, Suresh A and Condon JC: Elevated levels of uterine anti-apoptotic signaling may activate NFKB and potentially confer resistance to caspase 3-mediated apoptotic cell death during pregnancy in mice. Biol Reprod 85: 417-424, 2011.
48. Zeng W, Li H, Chen Y, Lv H, Liu L, Ran J, Sun X, Bieerkehazhi S, Liu Y, Li X, *et al*: Survivin activates NF-κB p65 via the IKKβ promoter in esophageal squamous cell carcinoma. Mol Med Rep 13: 1869-1880, 2016.
49. Eichner LJ, Perry MC, Dufour CR, Bertos N, Park M, St-Pierre J and Giguère V: miR-378(*) mediates metabolic shift in breast cancer cells via the PGC-1β/ERRγ transcriptional pathway. Cell Metab 12: 352-361, 2010.
50. Wang Y, Zhang X, Wang Z, Hu Q, Wu J, Li Y, Ren X, Wu T, Tao X, Chen X, *et al*: LncRNA-p23154 promotes the invasion-metastasis potential of oral squamous cell carcinoma by regulating GLUT-1-mediated glycolysis. Cancer Lett 434: 172-183, 2018.
51. Chen Y, Sun R, Han W, Zhang Y, Song Q, Di C and Ma D: Nuclear translocation of PDCD5 (TFAR19): An early signal for apoptosis? FEBS Lett 509: 191-196, 2011.